Journal of Applied Polymer Science

Iodine diffusion during iodine-vapor curing and its effects on the morphology of polycarbosilane/silicon carbide fibers

Junsung Hong,[1] Kwang-Youn Cho,[2] Dong-Geun Shin,[3] Jung-Il Kim,[4] Doh-Hyung Riu[1]

[1]Department of Materials Science and Engineering, Seoul National University of Science and Technology, Seoul 139-743, Republic of Korea

[2]Nano Convergence-Intelligence Material Team, Korea Institute of Ceramic Engineering and Technology, 233-5 Gasan-dong, Guemcheon-gu, Seoul 153-801, Republic of Korea

[3]Energy Efficient Materials Team, Korea Institute of Ceramic Engineering and Technology, 233-5 Gasan-dong, Guemcheon-gu, Seoul 153-801, Republic of Korea

[4]DACC Co., Ltd., Dukjingu, Jeon-Ju, Jeon-buk 561-844, Republic of Korea

Correspondence to: D.-H. Riu (E-mail: dhriu15@seoultech.ac.kr)

ABSTRACT: Iodine-vapor curing is used to produce continuous SiC fibers from polycarbosilane (PCS), but attempts to limit the uptake of oxygen during the curing process result in SiC fibers with different morphologies and pore types. The cause of this distinct transformation in the morphology of the fibers is determined in this study by tracing the distribution of iodine in PCS fibers cured either at a set temperature or for a given period. The results reveal that the final morphology of the fibers is dependent on the degree of iodine diffusion, or on the extent of their cross-linked area. Using this knowledge, fibers with three distinct morphologies are produced by controlling the curing conditions. Optimization of this curing process is shown to inhibit the formation of pores and retard the incorporation of oxygen, while still allowing the fibers to retain their cylindrical shape. © 2015 Wiley Periodicals, Inc. J. Appl. Polym. Sci. **2015**, *132*, 42687.

KEYWORDS:

Received 15 March 2015; accepted 29 June 2015

DOI: 10.1002/app.42687

INTRODUCTION

Silicon carbide (SiC) fibers, which are a useful reinforcement material for ceramic matrix composites, are typically fabricated from polycarbosilane (PCS) via a sequence of spinning, curing, and pyrolysis.[1–3] The curing stage of the manufacturing process plays a pivotal role in determining the final quality of the SiC fibers, as it not only prevents the PCS fibers from fusing together during pyrolysis, but also has a significant effect on their mechanical properties.[4–9] A number of different curing methods have therefore been developed, which include thermal oxidation curing,[4–6] γ-ray/electron-beam radiation curing,[7–10] chemical vapor curing (CVC) using halogenated hydrocarbons or unsaturated hydrocarbon vapors,[11–13] and CVC using BCl_3 and ammonia.[14,15]

A new CVC method involving the use of iodine (i.e., I-vapor curing) was recently reported[16] that offers several advantages over existing techniques, including a decrease in the curing temperature and the time required. This new method is based on a cross-linking mechanism, wherein the diffusion of iodine into the PCS fibers induces a transition state in the molecular bonds of the Si—C—H structure that allows weak bonds to cleave and recombine at relatively low temperatures. This results in cross-linked networks such as —Si—C—, —C═C— and —Si—O—Si—; the —Si—O—Si— structure is only observed on the fiber surface, with its concentration increasing in proportion to the curing temperature.[16] When fabricating high-grade SiC fibers, however, the oxygen incorporated during the curing process is considered an impurity.[6,8,17] Thus, in the case of high-grade SiC fibers, it is necessary to inhibit the incorporation of oxygen.

Here, we attempted to optimize the curing process by reducing the temperature and duration of the curing process, but doing so produced the synthesis of SiC fibers with different morphologies and pore types. Controlling the shape of the fibers is also an important consideration because of the fact that the mechanical properties and characteristic of the fibers are determined by their shape. Several shapes of SiC fiber have been previously reported, with these including SiC monofilaments with large diameters,[18] SiC films for microelectromechanical systems (MEMS) and optoelectronic devices,[19,20] SiC microtubes,[21] and hollow SiC fibers for membranes to be used under harsh conditions.[22,23] Since

Table I. Experimental Conditions and Morphology of the Fibers Obtained

Condition					
I-vapor curing			Pyrolysis		
Conc. (g L^{-1})[a]	Temp. (°C)	Time (h)	Temp. (°C)	Time (min)	Morphology[b]
0.15	100	1	1200	60	Oblong
	120				Oblong
	130				Hollow
	140				Circular
1.52	80	1	600	10	Oblong
		2			Hollow
		3			Circular

[a] Concentration in this table indicates the iodine weight per chamber volume, which represents the relative vapor pressure of iodine during curing.
[b] Morphologies of the fibers obtained are shown in Figures 1 and 3.

fabricating different SiC fiber shapes clearly has the potential to create new applications, this study looks at the fabrication of SiC fibers with different morphologies ranging from oblong to hollow to circular by controlling the temperature and time of curing. The mechanism behind the morphological transformation of these fibers is studied through observation of both the manner in which iodine diffuses into them, and the extent to which it diffuses (i.e., the degree of curing). In addition, the way in which the distribution of elements in PCS, including oxygen, is affected by iodine diffusion was investigated. From the results of this, an optimized step-wise curing process is proposed.

EXPERIMENTAL

Preparation of Precursor

PCS was synthesized through the thermal decomposition of 600 g of polydimethylsilane (TBMTech, Korea) mixed with 30 g of aluminum(III)-acetylacetonate (Sigma-Aldrich LLC, USA) and 6 g of γ-Al_2O_3 (used as a catalyst) in an autoclave.[16,24,25] The resulting PCS sample had an average molecular weight (M_w) of 2491 and a melting point of 180–210°C. The PCS sample was then melt-spun at approximately 230°C using a single-spinner apparatus to obtain PCS fibers with diameters of 25–35 μm.

Characterization of Morphology and Elemental Distribution

The as-spun PCS fibers were I-vapor cured[16] either at a set temperature or for a given time, and then subsequently pyrolyzed. For the temperature-dependent curing, 200 mg of the as-spun PCS fibers and 150 mg of iodine powder (Yakuri Pure Chemicals, Japan) were placed in a vial, which was kept in a 1 L glass chamber. This chamber was then heated to 100°C, 120°C, 130°C, or 140°C for 1 h in air in a furnace; the time taken to reach the target temperature was kept constant at 10 min. The

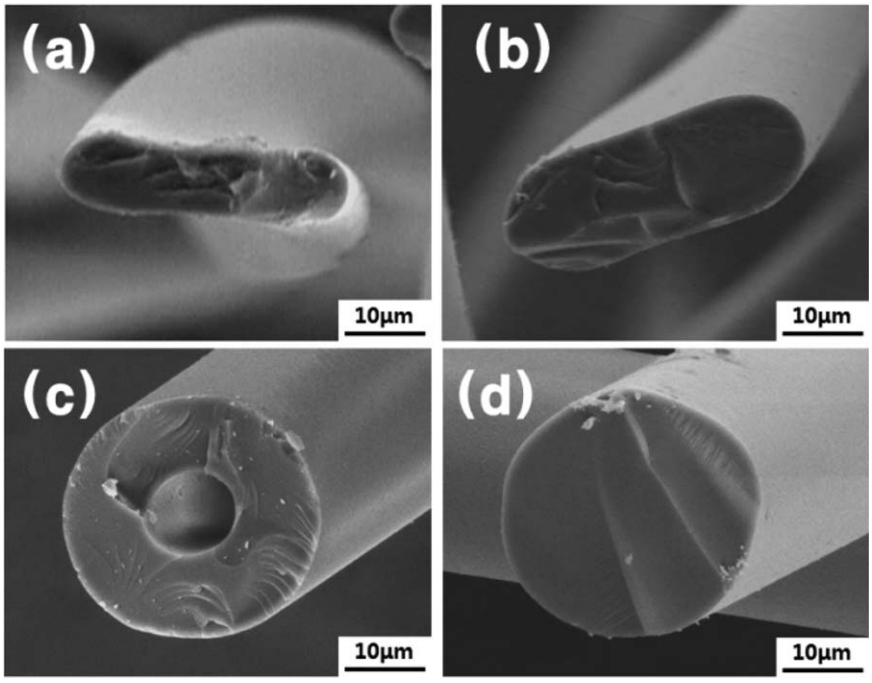

Figure 1. SEM images of SiC fibers pyrolyzed at 1200°C for 1 h in Ar after I-vapor curing at (a) 100°C, (b) 120°C, (c) 130°C, or (d) 140°C in air.

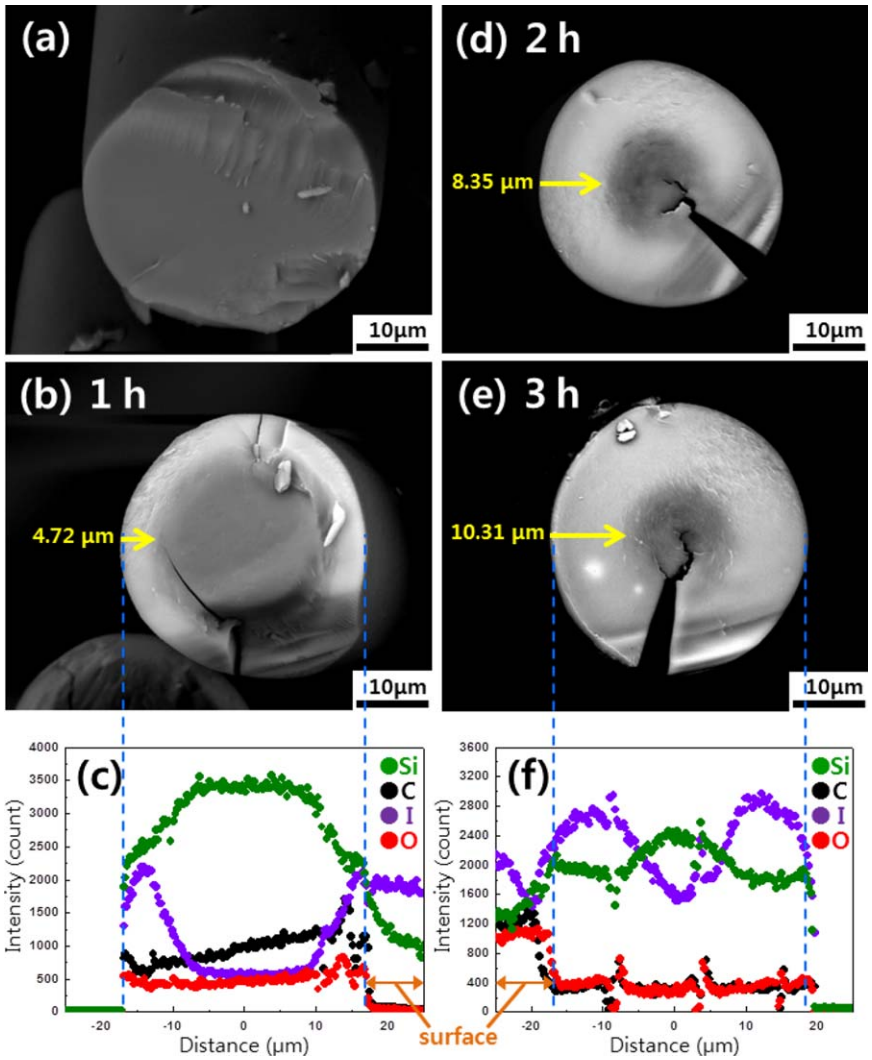

Figure 2. BSE images of (a) the as-spun PCS fibers and (b) the PCS fibers I-vapor cured at 80°C for 1, (d) 2, or (e) 3 h in air. Elemental line profiles of (c) the PCS fibers I-vapor cured at 80°C for 1 and (f) 3 h. [Color figure can be viewed in the online issue, which is available at wileyonlinelibrary.com.]

cured PCS fibers were then sintered at 1200°C (heating rate of 10°C min^{-1}) for 1 h in a furnace in Ar gas (flow rate of 1 L min^{-1}). The morphologies of the resulting fibers were observed using field-emission scanning electron microscopy (FESEM) (JSM-6700F, JEOL, Japan).

For the time-dependent curing, 30 mg of the PCS fibers and 50 mg of iodine powder were placed in a vial, which was kept in a 33 mL glass chamber. The chamber was then heated to 80°C in air for 1, 2, or 3 h; the heating rate was 5°C min^{-1}. The depth to which iodine diffused during this process and the elemental distributions of Si, C, and O in the resulting fibers were analyzed using a field-emission electron probe microanalyzer (FE-EPMA) (JXA-8500F, JEOL, Japan) and wavelength-dispersive spectroscopy (WDS). The time-dependently cured PCS fibers were then heated at 600°C for 10 min (heating rate of 10°C min^{-1}) to obtain semipyrolyzed fibers that were light brown; this allowed any pores present in the fibers to be observed with ease. The morphologies of the fibers and the inner pores formed in the fibers after the heat treatment were observed using optical microscopy (OM) (Eclipse Ti, Nikon, Japan), as well as using FESEM (JSM-6700F, JEOL, Japan).

Thermal Analysis

The formation of pores in the fibers was investigated further through thermogravimetric and differential thermal analyses (TG-DTA) (DTG-60H, Shimadzu, Japan), which were performed on PCS fibers I-vapor cured at 130°C for 1 h; i.e., under conditions considered optimal for ensuring that pores were produced in the cores of the fibers.

Monitoring of Iodine Diffusion

In order to trace the diffusion of iodine in the PCS fibers, the following samples were prepared: as-spun PCS fibers, PCS fibers I-vapor cured at 80°C for 30 min in air, and PCS fibers I-vapor cured at a series of temperatures (80°C, 120°C, and 150°C) for 30 min each in air. The cross-sections of these fibers were then probed using FE-EPMA (JXA-8500F, JEOL, Japan), in order to determine the distribution of iodine within each fiber type.

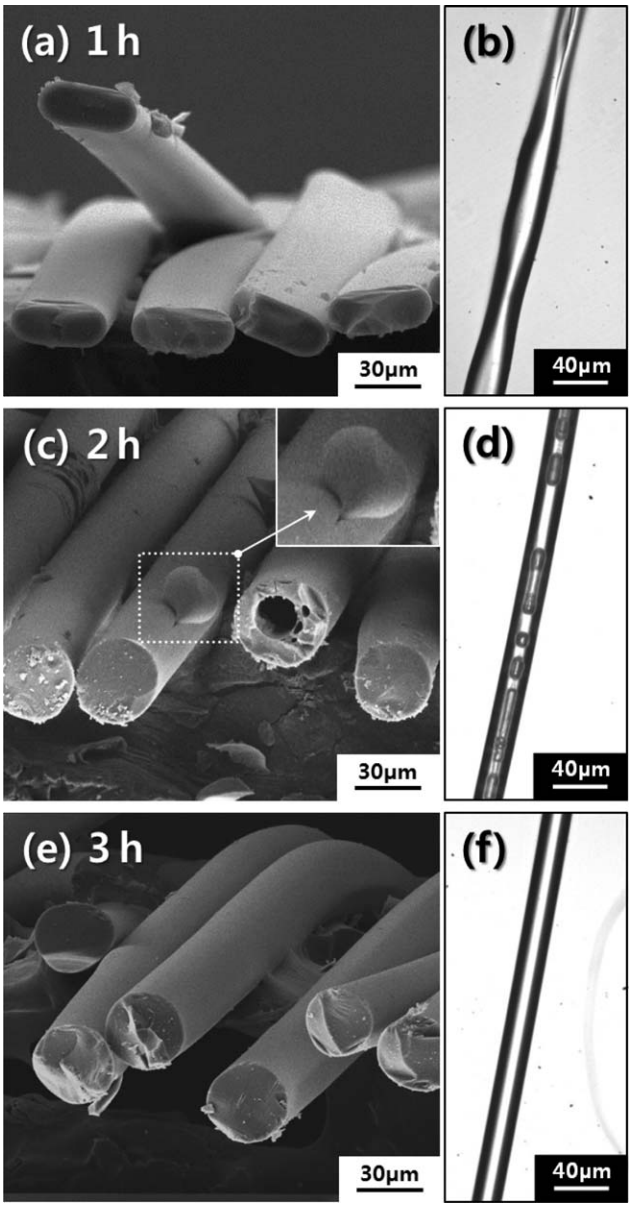

Figure 3. SEM and transmitted-light optical micrographs of PCS fibers slightly pyrolyzed at 600°C for 10 min after I-vapor curing at 80°C for (a,b) 1, (c,d) 2, or (e,f) 3 h in air.

RESULTS AND DISCUSSION

Dependence of Morphological Change on Curing Conditions

The curing and heat-treatment conditions used and the morphologies of the resulting fibers are listed in Table I. Figure 1 shows SEM images of the SiC fibers obtained via temperature-dependent curing and a subsequent heat-treatment. It can be seen from the images that curing at 100°C or 120°C resulted in oblong SiC fibers [Figure 1(a,b)], with those cured at 100°C tending to have a more flattened shape. Although these fibers did not seem to be perfectly cured, the sticking or tangling of filaments was not observed. Increasing the curing temperature to 130°C or 140°C resulted in circular fibers [Figure 1(c,d)], though those obtained at 130°C contained centered pores [Figure 1(c)].

Figure 2 shows backscattered electron (BSE) images and elemental line profiles of the time-dependently cured PCS fibers. It should be noted here that no cracks were seen during the initial observation. Thus, the cracks evident in these images were presumably caused by the thermal shock induced during the EPMA process.[26] That aside, three important things are evident from these images. Firstly, the concentration of oxygen within the fibers remained almost constant, while that on the surface concentration increased notably with time [Figure 2(c,f)]). This proved that oxygen infiltrated the fibers only at the surface level when the curing temperature was as low as 80°C, even though the treatment time was 3 h. Secondly, unlike oxygen, the iodine diffused further into the PCS fiber over time (Figure 2), suggesting that the diffusion of the two elements did not occur concurrently. The bright fiber rim in the BSE images was confirmed by the elemental line profiles to be an iodine-incorporating region [Figure 2(c,f)]. Finally, the concentration of silicon exhibited a tendency opposite to that shown by

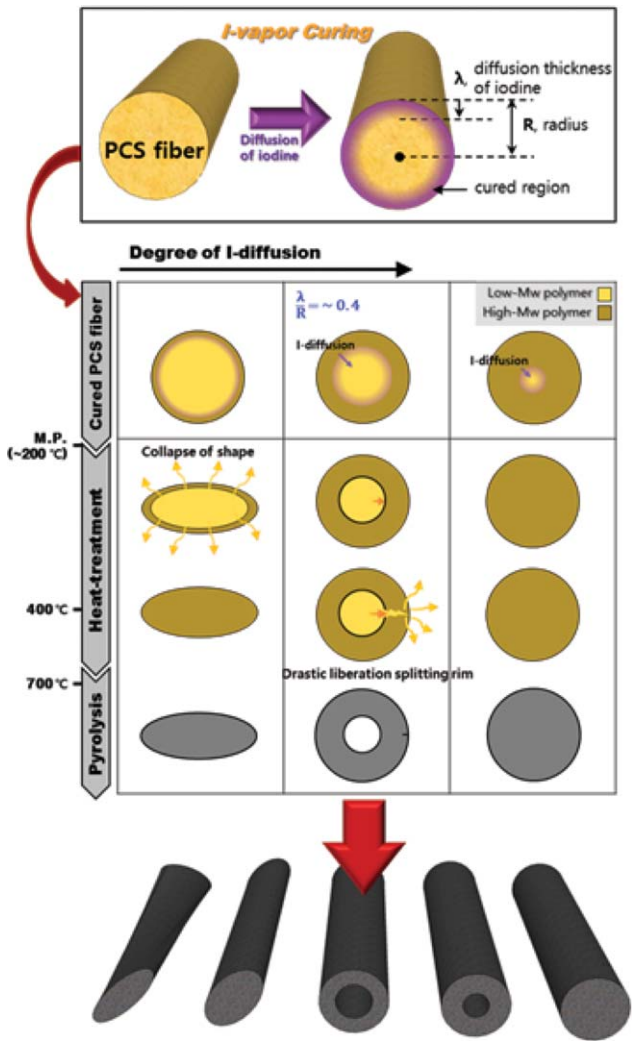

Figure 4. Schematic illustration showing the mechanism responsible for the morphological transformation of PCS fibers into three types of SiC fibers, depending on the curing level (or the degree of iodine diffusion). [Color figure can be viewed in the online issue, which is available at wileyonlinelibrary.com.]

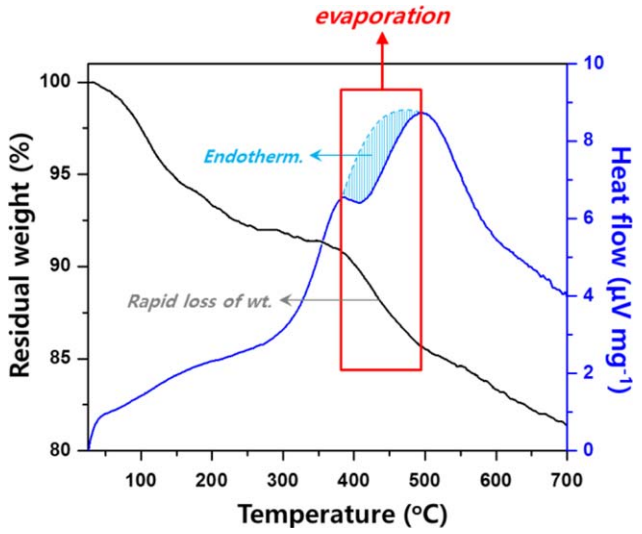

Figure 5. TG-DTA graph of the rim-cured PCS fibers obtained after I-vapor curing at 130°C for 1 h in air; the analysis conditions correspond to the optimal conditions for producing pores in the cores of the fibers during pyrolysis. [Color figure can be viewed in the online issue, which is available at wileyonlinelibrary.com.]

the iodine concentration [Figure 2(c,f)]; this was attributable to the release of oligomeric silanes during the curing process.[16]

Figure 3 shows SEM and OM images of the slightly pyrolyzed PCS fibers after time-dependent curing, with their corresponding iodine distributions given in Figure 2(b,d,e). As with the temperature-dependently cured fibers shown in Figure 1, these also exhibited morphologies ranging from oblong to hollow to circle. The oblong fibers, which were produced via curing for 1 h, appeared to be pressed during the heat treatment [Figure 3(a,b)]; however, they had a ~4.72 μm-thick cured layer that can be seen as a bright area in Figure 2(b). As these oblong SiC fibers have a morphology very similar to SiC films,[19,20] they may find application in MEMS and optoelectronic devices. The circular PCS fibers obtained via curing for 2 h, contained numerous cylindrical pores that varied in distribution and length [Figure 3(c,d)], despite having had a thicker cured layer ~8.35 μm in width [Figure 2(d)]. In terms of structure, these fibers were similar to the hollow carbon fibers (diameter of 110 μm) produced from poly(vinyl) alcohol fibers by Fatema *et al.* using a liquid iodine compound.[27] Although the pores were not interconnected, several of them appeared to have combined together to form one axial pore [Figure 3(d)], implying the possibility of continuous cylindrical pores forming in the fibers. Finally, since circular PCS fibers free of pores could be obtained after 3 h of curing, it can be concluded that altering the degree of curing (i.e., the extent of the cross-linked area or the degree of iodine diffusion into PCS) by changing either the curing temperature or time had a direct effect on the morphology of the fibers during pyrolysis.

Mechanism of Morphologic Transformation

On the basis of the results discussed in the previous section, we propose a mechanism to explain the morphological transformation of the PCS fibers into the three distinct types illustrated in Figure 4. With the first type, the skin-cured PCS fibers become oblong in shape, as it is difficult for the thin cured skin to maintain its original shape under the force of gravity during the heat treatment. However, as the fiber surface is densely cross-linked with a high concentration of Si—O—Si networks, the fibers have very stable skin and thus do not become entangled or stuck together. In the case of the second type, partial rim curing (when the ratio of λ/R, as illustrated in Figure 4, is approximately 0.4.) results in circular fibers with cylindrical pores. When the partially cured fibers are pyrolyzed at elevated temperatures, any uncured polymer remaining melts and vaporizes. Meanwhile, the cured rim does not fuse and therefore only barely retains its original circular shape, thereby allowing cylindrical pores to form in the fibers. Indeed, the small globular surface lump in Figure 3(c) appears to be released from the molten or vaporized polymer splitting the rim. The third type, normal circular fibers, is obtained when iodine diffuses deep into the near-core area of the fibers during the curing process.

The temperature at which pores were formed was determined by performing TG-DTA on the rim-cured PCS fiber (Figure 5). The exothermic peak between 300°C and 500°C in Figure 5 is the result of condensation among the molecules, which caused separation of the low-M_w hydrocarbons and increased the molecular weight of the sample.[28,29] With these facts in mind, the dent between 375°C and 485°C can be attributed to the vaporization of the sample; i.e., this was an endothermic reaction that resulted in rapid weight loss. In other words, 375–485°C represents the temperature range over which the cylindrical pores evolved and gases were released. The oblong fibers seen in Figure 3(a,b), however, did not form any pores. This is because the incompletely cross-linked rims and short center to surface distance in the oblong fibers, unlike the more fully cured fibers, facilitate the free movement of gas and subsequent shrinkage of the oblong fibers (Figure 4).

Optimization of the Curing Process

As the ultimate goal of this study was to obtain SiC fibers with a high tensile strength that can be used at high temperatures, it was essential that these fibers not only be circular and poreless but

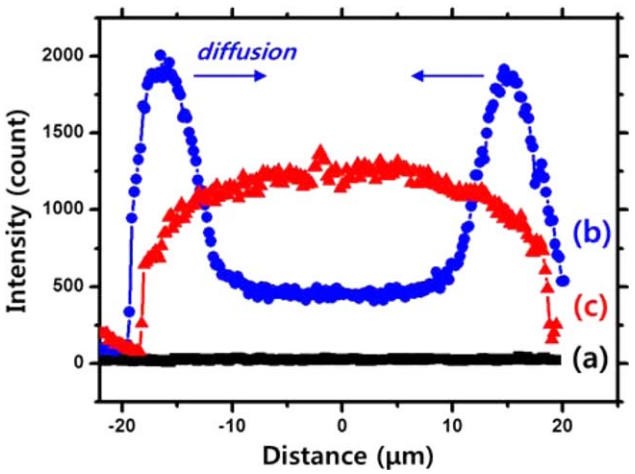

Figure 6. Line profiles of iodine in the cross-sections of (a) an as-spun PCS fiber, (b) a PCS fiber I-vapor cured at 80°C for 30 min in air, and (c) a PCS fiber I-vapor cured in air at a series of temperatures (80°C, 120°C, and 150°C) for 30 min each. [Color figure can be viewed in the online issue, which is available at wileyonlinelibrary.com.]

also have low oxygen content. Either high-temperature curing for a short period or low-temperature curing for a long duration could prevent pore formation; however, both these processes tend to involve significant oxygen uptake. To inhibit this oxygen incorporation, the curing conditions need to be optimized so as to achieve a balance between the curing time and temperature. In this regard, we suggest using a stepwise curing process that is performed at a series of different temperatures. Specifically, a low temperature should be used for the predeposition process, with this being followed by curing at a higher temperature to allow for iodine diffusion within a shorter period of time. Actually, as shown in Figure 6, a stepwise curing at 80°C, 120°C, and 150°C for 30 min each, ensures that the iodine diffuses into the cores of the fibers. As a result, the fibers are completely cured in a relatively short time, thus minimizing their uptake of oxygen from the air. The SiC fibers fabricated using this kind of process (i.e., heating at 80°C, 100°C, and 120°C) exhibited a tensile strength of 1.82 GPa and a Young's modulus of 189 GPa.[16]

CONCLUSIONS

The morphology of I-vapor-cured PCS fibers changes during pyrolysis, with circular PCS fibers transforming into either oblong fibers, pore-containing SiC fibers or circular SiC fibers. The final morphology of the fibers has been found to be determined by the extent of their cross-linked area; i.e., the extent of iodine distribution in the PCS fibers or their degree of iodine curing. This, in turn, is dependent on the curing temperature and time, as well as the partial pressure of iodine during the curing process. The results of this study suggest that it is possible to control the morphology of SiC fibers; however, further research is needed for this to be more effectively applied to small-diameter fibers. The EPMA analyses also demonstrate that when the curing temperature is low oxygen only infiltrates the fibers at a surface level, no matter how long it was treated. A stepwise approach to I-vapor curing has therefore been suggested as a practical means of controlling fiber morphology, but the characteristics of the SiC fibers with different morphologies should be further studied to determine what potential new applications they may have. In keeping with this goal, we are currently investigating the fabrication of hollow SiC fibers.

ACKNOWLEDGMENTS

This research was supported by a grant (Code# 10040046) from the Core Tech Material R&D Program of the Ministry of Trade, Industry and Energy (MOTIE), Republic of Korea.

Some of the results presented here are based on parts of author Junsung Hong's M.S. Thesis at Seoul National University of Science and Technology, January 2014.

REFERENCES

1. Yajima, S.; Hasegawa, Y.; Okamura, K.; Matsuzawa, T. *Nature* **1978**, *273*, 525.
2. Ishikawa, T.; Kohtoku, Y.; Kumagawa, K.; Yamamura, T.; Nagasawa, T. *Nature* **1998**, *391*, 773.
3. Ishikawa, T.; Kajii, S.; Matsunaga, K.; Hogami, T.; Kohtoku, Y.; Nagasawa, T. *Science* **1998**, *282*, 1295.
4. Okamura, K.; Sato, M.; Hasegawa, Y. *J. Mater. Sci. Lett.* **1983**, *2*, 769.
5. Ichikawa, H.; Teranishi, H.; Ishikawa, T. *J. Mater. Sci. Lett.* **1987**, *6*, 420.
6. Chu, Z. Y.; Feng, C. X.; Song, Y. C.; Wang, Y. D.; Li, X. D.; Xiao, J. Y. *Trans. Nonferrous Met. Soc. China* **2002**, *12*, 894.
7. Takeda, M.; Imai, Y.; Ichikawa, H.; Kasai, N.; Seguchi, T.; Okamura, K. *Compos. Sci. Technol.* **1999**, *59*, 793.
8. Takeda, M.; Sakamoto, J.-i.; Imai, Y; Ichikawa, H. *Compos. Sci. Technol.* **1999**, *59*, 813.
9. Ichikawa, H. *J. Ceram. Soc. Jpn.* **2006**, *114*, 455.
10. Okamura, K.; Seguchi, T. *J. Inorg. Organomet. Polym.* **1992**, *2*, 171.
11. Hasegawa, Y. *Compos. Sci. Technol.* **1994**, *51*, 161.
12. Li, W.; Song, Y. C.; Mao, X. H. *J. Mater. Sci.* **2006**, *41*, 7011.
13. Mao, X. H.; Song, Y. C.; Li, W.; Yang, D. X. *J. Appl. Polym. Sci.* **2006**, *105*, 1651.
14. Atwell, W. H.; Bujalski, D. R.; Joffre, E. J.; Legrow, G. E.; Lipowitz, J.; Rabe, J. A. (Dow Corning Corporation). EP 0435065 B1, Mar 15, 1995.
15. Deleeuw, D. C.; Lipowitz, J. Lu, (Dow Corning Corporation). EP 0438117 B1, Aug 19, **1998**.
16. Hong, J.; Cho, K. Y.; Shin, D. G.; Kim, J. I.; Oh, S. T.; Riu, D. H. *J. Mater. Chem. A* **2014**, *2*, 2781.
17. Jacobson, N. S.; Opila, E. J. *Metall. Mater. Trans. A* **1993**, *24*, 1212.
18. Andreas, N. *J. Eur. Ceram. Soc.* **2014**, *34*, 1487.
19. Yao, R.; Feng, Z.; Yu, Y.; Li, S.; Chen, L.; Zhang, Y. *J. Eur. Ceram. Soc.* **2009**, *29*, 2079.
20. Yao, R.; Feng, Z.; Zhang, B.; Zhao, H.; Yu, Y.; Chen, L.; Zhang, Y. *Opt. Mater.* **2011**, *33*, 635.
21. Colombo, P.; Perini, K.; Bernardo, E.; Capelletti, T.; Maccagnan, G. *J. Am. Ceram. Soc.* **2003**, *86*, 1025.
22. Shin, D.-G.; Kong, E.-B.; Cho, K.-Y.; Kwon, W.-T.; Kim, Y.; Kim, S.-R.; Hong, J.; Riu, D.-H. *J. Kor. Ceram. Soc.* **2013**, *50*, 301.
23. de Wit, P.; Kappert, E. J.; Lohaus, T.; Wessling, M.; Nijmeijer, A.; Benes, N. E. *J. Membrane Sci.* **2015**, *475*, 480.
24. Riu, D.-H.; Kim, Y.; Shin, D.-G.; Park, H.-S.; Lim, D.-W.; Yoon, C.-S. Korean Patent 10–0684649, **2007**.
25. Shin, D.-G.; Kong, E.-B.; Riu, D.-H.; Kim, Y.; Park, H.-S.; Kim, H.-E. *J. Kor. Ceram. Soc.* **2007**, *44*, 393.
26. Goldstein, J. I.; Newbury, D. E.; Echlin, P.; Joy, D. C.; Romig, A. D., Jr.; Lyman, C. E.; Fiori, C.; Lifshin, E. Scanning Electron Microscopy and X-Ray Microanalysis, 2nd ed.; Plenum: New York, **1992**.
27. Fatema, U. K.; Tomizawa, C.; Harada, M.; Gotoh, Y. *Carbon* **2011**, *49*, 2158.
28. Hasegawa, Y.; Okamura, K. *J. Mater. Sci.* **1983**, *18*, 3633.
29. Matthews, S.; Edirisinghe, M. J.; Folkes, M. J. *Ceram. Int.* **1999**, *25*, 49.